

**OPEN ACCESS**

## La<sub>2/3</sub>Sr<sub>1/3</sub>MnO<sub>3</sub> thin films deposited by laser ablation on lithium niobate substrates

To cite this article: I T Gomes *et al* 2010 *J. Phys.: Conf. Ser.* **200** 052007

View the [article online](#) for updates and enhancements.

### You may also like

- [Strain induced modulation of the correlated transport in epitaxial Sm<sub>0.5</sub>Nd<sub>0.5</sub>NiO<sub>3</sub> thin films](#)  
L Zhang, H J Gardner, X G Chen et al.
- [Double-doping Effect on Structural and Magnetic Properties of Perovskite Lanthanum Manganite](#)  
Farid F. Hanna and Peter N. G. Ibrahim
- [Oxygen Permeability and Ionic Conductivity of Perovskite-Related La<sub>0.3</sub>Sr<sub>0.7</sub>Fe \(Ga\)O<sub>3</sub>](#)  
V. V. Kharton, A. A. Yaremchenko, A. P. Viskup et al.

## **La<sub>2/3</sub>Sr<sub>1/3</sub>MnO<sub>3</sub> thin films deposited by laser ablation on lithium niobate substrates**

**I T Gomes<sup>1</sup>, A M Pereira<sup>2</sup>, J P Araújo<sup>2</sup>, A M L Lopes<sup>3</sup>, M E Braga<sup>2</sup>, B G Almeida<sup>1</sup>**

<sup>1</sup>Departamento de Física, Universidade do Minho, Campus de Gualtar, 4710-057 Braga, Portugal

<sup>2</sup>Departamento de Física and IFIMUP-IN, Institute of Nanoscience and Nanotechnology, Universidade do Porto, Rua do Campo Alegre 687, 4169-007 Porto, Portugal

<sup>3</sup>Centro de Física Nuclear, Universidade de Lisboa, Av. Prof. Gama Pinto 2, 1649-003 Lisboa, Portugal

isabelgomes@fisica.uminho.pt

**Abstract.** The structural, magnetic and transport properties of La<sub>2/3</sub>Sr<sub>1/3</sub>MnO<sub>3</sub> thin films, prepared by laser ablation on LiNbO<sub>3</sub> substrates, have been characterized for different temperatures and applied magnetic fields. The deposited films have grown highly oriented, with a (111) preferred growth direction. Their lattice parameter was  $a = 3.86 \text{ \AA}$ . From the temperature dependence of the magnetization and of the electrical resistivity their Curie ( $T_C$ ) and metal-insulator ( $T_{MI}$ ) transition temperatures were determined ( $T_C \sim 360 \text{ K}$ ,  $T_{MI} \sim 260 \text{ K}$ ). Spin-dependent tunnelling across grain boundaries was found to dominate the behaviour of the transport properties of the La<sub>2/3</sub>Sr<sub>1/3</sub>MnO<sub>3</sub> thin films, on the studied temperature region.

### **1. Introduction**

Colossal magnetoresistive manganites have been attracting much scientific and technological interest [1-3]. On the doped perovskite-type lanthanum manganites (La<sub>1-x</sub>A<sub>x</sub>)MnO<sub>3</sub> (A = divalent alkaline-earth ions) a ferromagnetic coupling between the Mn ions develops in the concentration range  $x = 0.2-0.6$ , due to the double exchange mechanism [3]. Above the Curie temperature ( $T_C$ ), charge transport is thermally activated and the electrical resistivity is high. Near  $T_C$ , the electrical resistivity has a maximum and then drops to a metallic-like character below a characteristic metal-insulator transition temperature  $T_{MI}$ . Upon application of a magnetic field, the resistivity of these manganites strongly decreases, i.e., they present colossal magnetoresistance (CMR).

In the particular case of La<sub>2/3</sub>Sr<sub>1/3</sub>MnO<sub>3</sub> (LSMO) the Curie temperature attains the highest value for these materials, reaching 380 K. Combined with its CMR characteristics, this high  $T_C$  makes LSMO a promising material for room-temperature magnetic sensors, recording devices or bottom electrode in the fabrication of ferroelectric memories [2,3]. In LSMO thin films it is known that lattice mismatch between the manganite and the substrate induces strain in the films, changing Mn-O bond lengths and Mn-O-Mn bond angles inside the unit cell. This then makes their structural (unit cell distortion), transport (stabilization of the metallic phase) and magnetic properties (increased magnetic anisotropy,

$T_C$  changes) strongly influenced by the substrate characteristics [3]. In this regard, lithium niobate ( $\text{LiNbO}_3$ ) presents a rich variety of favourable properties for integrated and waveguide optics and is widely used in electro-optical devices [4]. It is ferroelectric up to  $1210^\circ\text{C}$  and in the ferroelectric phase it presents a trigonal crystal structure ( $R3c$  space group), with  $a = 5.148 \text{ \AA}$  and  $c = 13.863 \text{ \AA}$ . In its  $z$ -cut form  $a$  is in-plane and its value is similar to the diagonal of the LSMO pseudo-cubic unit cell, reducing film-substrate mismatch. Thus, in this work, LSMO thin films have been deposited on  $\text{LiNbO}_3$  substrates in order to characterize their structural, magnetic and transport properties.

## 2. Experimental details

The LSMO thin films were prepared by pulsed laser ablation on  $z$ -cut  $\text{LiNbO}_3$  crystal substrates. The depositions were done with a KrF excimer laser (wavelength  $\lambda = 248 \text{ nm}$ ), at a fluence of  $2 \text{ J/cm}^2$ , a  $3\text{Hz}$  repetition rate and a pulse duration of  $25 \text{ ns}$ . The oxygen pressure during preparation was  $0.5 \text{ mbar}$  and the substrate temperature was  $720^\circ\text{C}$ . After the deposition, the films were cooled down to room temperature at atmospheric oxygen pressure.

For the laser ablation targets, polycrystalline samples of  $\text{La}_{2/3}\text{Sr}_{1/3}\text{MnO}_3$  were prepared by the gel combustion method. Stoichiometric amounts of  $\text{La}_2\text{O}_3$ ,  $\text{SrCO}_3$ , and  $\text{MnCO}_3$  were used as starting materials. These oxides/carbonates were converted into metal nitrates by adding nitric acid and dissolved in distilled water to obtain a clear solution. Citric acid (CA) and urea were used as fuel/complexing agents with a molar ratio of  $[\text{urea}]/[\text{salts}] = 3$  and  $[\text{CA}]/[\text{salts}] = 2$ . By adding ammonia the pH of solution was adjusted to  $6.5$ . Subsequently, the solution was heated with stirring to evaporate most of the solvent water. The resultant gel precursor was then decomposed at about  $250^\circ\text{C}$  and a black precursor powder was obtained. In order to get the laser ablation targets this powder was ground and pelletized and then annealed at temperatures from  $500^\circ\text{C}$  to  $1400^\circ\text{C}$ , during 1 day.

The structure was analyzed by X-ray diffraction (XRD) with a Siemens D5000 diffractometer using  $\text{Cu K}_\alpha$  radiation. The magnetic properties were measured with a Quantum Design MPMS SQUID magnetometer in the  $5 - 380 \text{ K}$  temperature range. The electrical resistivity measurements were performed in the  $10 - 300 \text{ K}$  temperature range, with the standard four probe in-line technique. The magnetoresistance was measured with the applied field parallel to the electrical current, in the  $77 - 300 \text{ K}$  temperature range.

## 3. Results and discussion

Figure 1a) shows the XRD spectrum of an LSMO thin film deposited on a  $\text{LiNbO}_3$  substrate. The observed diffraction peaks were fitted with gaussian functions in order to determine the peak positions

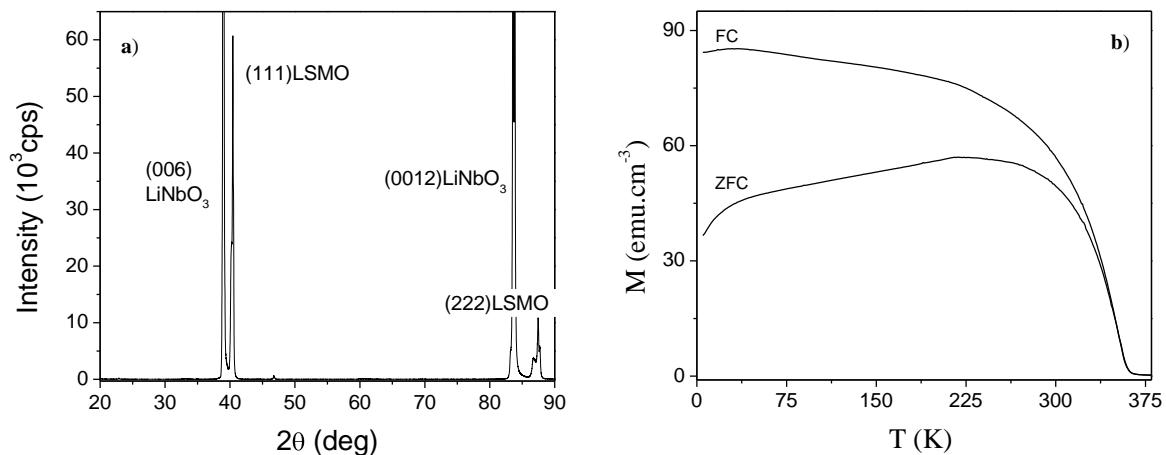


**Figure 1:** (a) X-ray diffraction spectrum measured on an LSMO thin film deposited by pulsed laser ablation on a  $\text{LiNbO}_3$  substrate. In (b) is the corresponding temperature dependence of the magnetization, obtained after zero-field cooling (ZFC) and after field cooling (FC) with a  $50 \text{ Oe}$  applied magnetic field.

and widths. The films are composed by LSMO ( $\text{La}_{2/3}\text{Sr}_{1/3}\text{MnO}_3$ ) and have grown with their unit cell tilted relative to the plane of the films, presenting a [111] orientation along the growth direction. The pseudocubic lattice parameter, determined from the (111) peak position, was  $a_{\text{film}} = 3.86 \text{ \AA}$ . The grain size, as determined from the width of the (111) XRD peak using the Scherrer equation [5], was  $\sim 235 \text{ nm}$ .

The lattice mismatch along the interface between the z-cut  $\text{LiNbO}_3$  substrate and the LSMO film is defined as  $\delta = 100\% \times (a_S - d_{f,\text{bulk}})/a_S$ , where  $d_{f,\text{bulk}}$  is the length of the film unit cell along the interface and  $a_S$  is the  $\text{LiNbO}_3$  lattice parameter ( $a_S = 5.148 \text{ \AA}$ ). On a [001]-oriented LSMO film  $d_{f,\text{bulk}} = a_{\text{bulk}}$  (pseudocubic lattice parameter of LSMO:  $a_{\text{bulk}} = 3.873 \text{ \AA}$ ) that would give  $\delta = 24.8\%$ . This value is very high, hindering the formation of an [001] oriented growth of the film. However, for [111] growth and considering that  $d_{f,\text{bulk}}$  is the diagonal of the pseudo-cube's face,  $\sqrt{2}a_{\text{bulk}}$ , the mismatch becomes  $\delta = -6.4\%$ , which is below the mismatch value between LSMO and the widely used  $\text{MgO}$  substrate [3]. This then favors a [111] LSMO preferential growth direction on  $\text{LiNbO}_3$  substrates, as observed on our films.

Figure 1b) shows the temperature dependence of the magnetization  $M(T)$ . The zero-field-cooled curve (ZFC) was obtained by measuring  $M(T)$  after cooling the sample from 380 K down to 5 K under no applied magnetic field. The field-cooled curve (FC) was obtained after initially cooling the sample with an applied field of  $H = 50 \text{ Oe}$  and then performing the measurements on heating. A paramagnetic-to-ferromagnetic phase transition is observed at a Curie temperature of  $T_C \sim 360 \text{ K}$ . Below  $\sim 330 \text{ K}$  the ZFC and FC curves separate, indicating an irreversibility associated with the presence of magnetically disordered clusters on the films[2].

On the other hand, the electrical resistivity, shown in figure 2a), initially rises, attaining a maximum at the metal-insulator transition temperature  $T_{\text{MI}} \sim 260 \text{ K}$ . Then, below  $T_{\text{MI}}$  and down to  $\sim 50 \text{ K}$ , it changes to a metallic-like behaviour characteristic of the ferromagnetic phase. Below 50 K the resistivity increases again suggesting that grain boundary (GB) scattering plays an important role in the transport properties of the films. In fact, this behaviour, along with the slightly smaller Curie temperature as compared to the bulk LSMO ( $T_{C,\text{bulk}} = 380 \text{ K}$ ), is due to the presence of magnetic inhomogeneities, where clusters of the metallic phase are mixed in a magnetically disordered insulating matrix, hindering the formation of the fully metallic phase.

Figure 2b) shows the magnetoresistance  $\text{MR} = [\rho(H) - \rho_0]/\rho_0$  of the LSMO films, measured in the temperature range 77 – 300 K. Its behaviour and magnitude are similar to the ones reported on (111)-LSMO films grown on strontium titanate covered Si substrates [6]. An initial sharp decrease of the

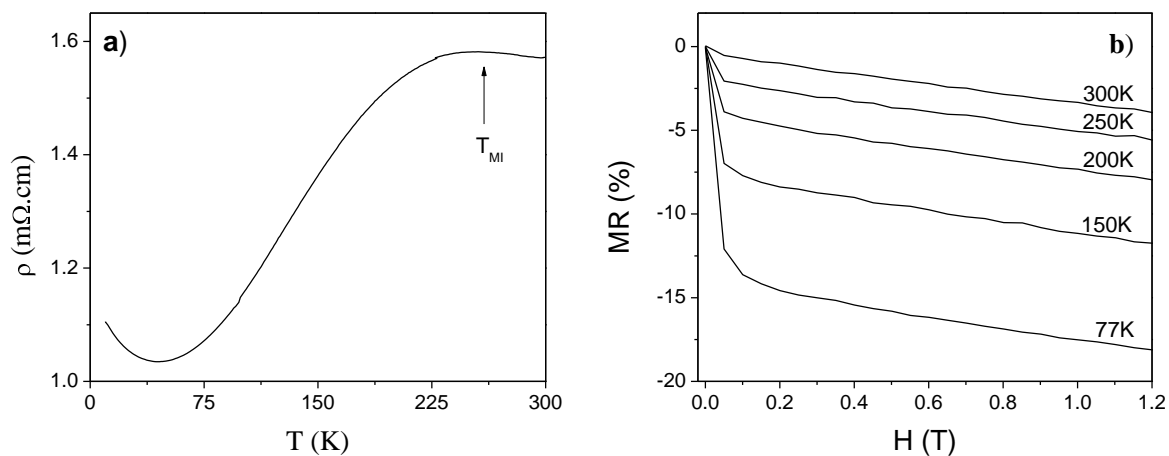


**Figure 2:** (a) Temperature dependence of electrical resistivity and (b) magnetoresistance measured on a laser ablation deposited LSMO thin film.

MR is observed at low fields ( $H < 0.1$  T), due to spin-dependent tunnelling across grain boundaries [2,7]. Then, beyond 0.1 T, the MR presents an approximately linear dependence with increasing magnetic field. Also, as the temperature increases, the magnitude of the MR decreases, particularly the low field magnetoresistance. In a manganite the grain boundary region has a significant amount of local spins [8]. Additionally, LSMO presents a strong spin polarization, due to the complete separation of the relatively narrow and almost fully occupied majority carrier conduction band (“spin-up”), from the minority band, induced by large Hund’s and exchange energies [3,7]. Then, if no spin-flip occurs (such as at low temperatures) the transmission of electrons across the grain boundaries has lower (higher) probability for electrons with spins parallel (antiparallel) to the magnetization of the grain. At  $H = 0$ , where the orientational disorder of the magnetization of the grains is the most pronounced, the resistivity is high. On the other hand, if the grains magnetic moments are fully aligned the resistivity is low, due to the transmission of the minority spin electrons across grain boundaries.

At low  $H$ , the magnetic moments of the grains progressively align with increasing applied magnetic field, as the magnetization increases towards saturation. Consequently, the initial strong decrease of the magnetoresistance measured on the thin films (figure 2b) is due to the increase of their magnetization, as it approaches its saturation value at each temperature. On the other hand, at higher magnetic fields ( $H > 0.1$  T), local spins inside the GB continue to rotate towards  $H$  further increasing spin alignment and, thus, contributing to a further decrease of the magnetoresistance. The almost linear decrease of the magnetoresistance at high magnetic fields is then associated with a GB susceptibility  $\chi_B$ . The reduction of the magnetoresistance with increasing temperature is due to the corresponding decrease of the films magnetization as well as the increased spin-flip scattering and inelastic tunnelling (with loss of spin-polarization) [8], as observed on the measured thin films.

#### 4. Conclusions

$\text{La}_{2/3}\text{Sr}_{1/3}\text{MnO}_3$  thin films have been deposited by laser ablation on  $\text{LiNbO}_3$  substrates and their structural, magnetic and transport properties have been characterized. They have grown highly oriented, with a (111) preferred growth direction. From the temperature dependence of the electrical resistivity and magnetization the Curie and metal-insulator transition temperatures were determined. Spin-dependent grain boundary scattering was revealed to give an important contribution to the transport properties of the thin films, inducing a strong decrease of the resistance with the magnetic field, particularly at low  $H$ . As the temperature increased, the magnetization of the samples decreased while spin-flip scattering increased. This then induced a corresponding reduction of the spin-dependent scattering contribution on the transport properties of the films.

**Acknowledgments:** I.T. Gomes gratefully acknowledges a PhD grant from Fundação para a Ciência e Tecnologia (SFRH/BD/36348/2007).

#### References

- [1] Dagotto E 2002 *Nanoscale phase separation and colossal magnetoresistance* (Berlin: Springer)
- [2] Dorr K 2006 *J. Phys. D: Appl. Phys.* **39** R125
- [3] Haghiri-Gosnet A-M and Renard J-P 2003 *J. Phys. D: Appl. Phys.* **36** R127
- [4] Wooten E L, Kissa K M, Yi-Yan A, Murphy E J, Lafaw D A, Hallemeier P F, Maack D, Attanasio D V, Fritz D J, McBrien G J and Bossi D E 2000 *IEEE J. Sel. Top. Quant. Electron.* **6** 69
- [5] Warren B E 1990 *X-Ray Diffraction* (New York: Dover Publications)
- [6] Fontcuberta J, Bibes M, Martinez B, Trtik V, Ferrater C, Sanchez F and Varela M 1999 *Appl. Phys. Lett.* **74** 1743
- [7] Hwang H Y, Cheong S-W, Ong N P and Batlogg B 1996 *Phys. Rev. Lett.* **77** 2041
- [8] Sun H, Yu K W and Li Z Y 2003 *Phys. Rev. B* **68** 054413